Characterization of surface oxide films on titanium and bioactivity

B. FENG[1,2]*, J. Y. CHEN[1], S. K. QI[3], L. HE[3], J. Z. ZHAO[3], X. D. ZHANG[1]
[1]*Engineering Research Center in Biomaterials, Sichuan University, Chengdu 610064, China*
[2]*Department of Material Science and Engineering, Sichuan University of Science and Technology, Chengdu 610039, China*
[3]*Lanzhou Institute of Chemical Physics, Chinese Academy of Sciences, Lanzhou 730000, China*
E-mail: fengbh@263.net or nic7500@scu.edu.cn

Biological properties of titanium implant depend on its surface oxide film. In the present study, the surface oxide films on titanium were characterized and the relationship between the characterization and bioactivity of titanium was studied. The surface oxide films on titanium were obtained by heat-treatment in different oxidation atmospheres, such as air, oxygen and water vapor. The bioactivity of heat-treated titanium plates was investigated by immersion test in a supersaturated calcium phosphate solution. The surface roughness, energy morphology, chemical composition and crystal structure were used to characterize the titanium surfaces. The characterization was performed using profilometer, scanning electronic microscopy, ssesile drop method, X-ray photoelectron spectroscopy, common Bragg X-ray diffraction and sample tilting X-ray diffraction. Percentage of surface hydroxyl groups was determined by X-ray photoelectron spectroscopy analysis for titanium plates and density of surface hydroxyl groups was measured by chemical method for titanium powders. The results indicated that heat-treatment uniformly roughened the titanium surface and increased surface energy. After heat-treatment the surface titanium oxide was predominantly rutile TiO_2, and crystal planes in the rutile films preferentially orientated in (1 1 0) plane with the highest density of titanium ions. Heat-treatment increased the amount of surface hydroxyl groups on titanium. The different oxidation atmospheres resulted in different percentages of oxygen species in TiO_2, in physisorbed water and acidic hydroxyl groups, and in basic hydroxyl groups on the titanium surfaces. The immersion test in the supersaturated calcium phosphate solution showed that apatite spontaneously formed on to the rutile films. This revealed that rutile could be bioactivated. The analyses for the apatite coatings confirmed that the surface characterization of titanium has strong effect on bioactivity of titanium. The bioactivity of the rutile films on titanium was related not only to their surface basic hydroxyl groups, but also to acidic hydroxyl groups, and surface energy. Heat-treatment endowed titanium with bioactivity by increasing the amount of surface hydroxyl groups on titanium and its surface energy.

1. Introduction

Titanium implants are increasingly used in dentistry and orthopedics due to their excellent biocompatibility and mechanical properties. The biocompatibility of titanium may be attributed to its surface oxide film. The titanium oxide film formed naturally in air is dense and stable anatase TiO_2 with a thickness of about a few nonameters, which leads to high corrosion resistance of titanium. But titanium is usually bioinert and integration between titanium and tissue is a morphological connection, even if a direct bone-implant contact called osteointegration could be formed [1–3]. There have been considerable efforts for improving the bioactivity of titanium. Besides coating Ca-P layer, modifying the natural oxide film is also a promising way. It has been reported that anatase film prepared by electrochemical process or sol–gel method could attract calcium and phosphate ions from physiological environment to form an apatite coating, thus showed bioactivity [4, 5]. Many other studies also showed that titanium might be bioactivated by surface modification and the bioactivity of titanium depends on properties of titanium surface [6–8]. This study hopes to enhance the understanding of the relationship between the surface characteristics of titanium with its bioactivity. For this purpose, rutile surface films with different characteristics were fabricated by heat-treatment in

*Author to whom all correspondence should be addressed.

different oxidation atmospheres. The morphology, chemical composition, crystal structure, surface roughness, surface energy and density of surface hydroxyl groups of the rutile films were investigated by scanning electron microscopy, X-ray photoelectron spectroscopy, X-ray diffraction, profilography, contact angle goniometry and chemical method respectively and used to characterize the rutile films. The deposition test of calcium and phosphate ions on the surface was carried out in a supersaturated calcium phosphate solution in order to investigate the effect of the characteristics of the rutile films on the bioactivity of titanium. The results indicated that the rutile surface films could also endow titanium with bioactivity and the density of surface hydroxyl $(OH)_S$ groups and surface energy on the films were very important factors for the bioactivity of titanium surface.

2. Materials and methods

2.1. Sample preparation

2.1.1. Heat-treatment

Commercially pure titanium plates of $10 \times 10 \times 2\,mm^3$ in size with a small hand successively were wet abraded to 800 grit alumina paper, washed in actone, alcohol and deionized water, and dried at ambient temperature. The plates were then divided into four groups: S – as-received; H – heated at 600 °C for 30 min in air; X – heated at 600 °C for 30 min in the oxygen (90%) current with 0.5 L/min; W – heated at 600 °C for 30 min in the water vapor with $1.13–1.15 \times 10^5$ Pa. Following heat-treatment the samples were cooled to ambient temperature in heating devices.

2.1.2. Ca-P deposition on heat-treated titanium

After heat-treatment, each of the plates was tied with a cotton thread on the handle of the plate, and then vertically immersed in 20 ml SCP with pH 7.40 at 37 °C for 10 days. The ion concentrations of SCP were Ca^{2+} 3.10 mM, HPO_4^{2-} 1.86 mM, Na^+ 136.8 mM, Cl^- 144.5 mM and K^+ 3.71 mM. The solution was refreshed every other day. The vertical hanging of the samples was to exclude any artifact arising from sedimentation in the supersaturated solution. Immersed samples SS, HS, XS and WS corresponded to S, H, X and W. After 10 days, the plates were removed from SCP, washed thoroughly with deionized water and dried at ambient temperature.

2.2. Surface characterization

2.2.1. Surface roughness and morphology analyses

The surface roughness of the titanium plates was measured by a profilometer (Surtronic 3, Talor Ltd. Co. England).

The morphology of the surface and cross-section of the samples were observed by scanning electron microscopy (SEM). The samples for observation of cross-section were prepared by polishing the lateral areas of titanium plates before and after immersion in SCP.

2.2.2. Surface energy measurement

Contact angles of test liquids on the titanium plates were measured using a contact angle goniometer (JY-82, China) by a sessile drop method. The six test liquids are ethylene glycol (surface energy $\gamma = 48.3\,mJ/m^{-2}$) glycerol ($\gamma = 63.4\,mJ/m^{-2}$), double-distilled water ($\gamma = 72.8\,mJ/m^{-2}$), formamide ($\gamma = 58.2\,mJ/m^{-2}$), tritolyl phosphate ($\gamma = 40.9\,mJ/m^{-2}$), diiodomethane ($\gamma = 50.8\,mJ/m^{-2}$). The surface energy values of the samples were obtained from the plots of the Owens–Wendt–Kaeble's equation [9, 10]:

$$\gamma_{LV}(1 + \cos\theta) = 2(\gamma_L^d \cdot \gamma_s^d)^{1/2} + 2(\gamma_L^p \cdot \gamma_s^p)^{1/2} \quad (1)$$

where, subscripts L and S represent solid and liquid surfaces respectively, γ^d stands for dispersion component of total surface energy (γ) and γ^p is polar component, γ may be expressed as the sum of dispersion component and polar component:

$$\gamma = \gamma^d + \gamma^p \quad (2)$$

2.2.3. Measurement of density of hydroxyl groups on titanium surface (ρ_{OH})

Because the surface area of the titanium plate is very small and the amount of surface hydroxyl $(OH)_s$ groups on titanium is much lower, commercially pure titanium powder with 70–80 μm diameter was used for measuring the ρ_{OH} on the titanium surfaces. The same heat-treatments for the plates were used for the powder. After heat-treatment, powder samples SP, WP, HP and XP corresponded to S, W, H and X. The measuring procedure has been described in detail elsewhere [11, 12]. The outline is given below.

The titanium powders were immersed in a mixture of 1.6 M ammonium chloride solution and 0.13 M zinc chloride solution with pH 6.9 at ambient temperature for 10 min. During immersion active hydroxyl groups on the titanium surfaces were exchanged for zinc ions in the ratio of $Zn^{2+}: OH^- = 1:2$. After being filtered and rinsed thoroughly with deionized water, the powders were immersed in deionized water for 10 min to remove non-adsorbed species. The filtered, rinsed and dried powders were immersed in 2.42 M nitric acid for 10 min to release zinc ions into nitric acid solution. The concentration of zinc ions in the solution was measured using an inductively coupled plasma atomic emission spectrometer (ICP-AES) (Optima 3000 XLICP America). The number of active $(OH)_s$ groups on the surfaces was obtained by doubling the number of zinc ions.

The specific surface areas of the powders were determined by BET method with an auto-adsorber (Digisirb2600, Micromeritics, America) in order to calculate the ρ_{OH}.

2.2.4. Surface composition and crystal structure analyses

The chemical composition of the titanium surfaces was determined by X-ray photoelectron spectroscopy (XPS, PHI-5702 XPS-AES, America) with MgKα radiation.

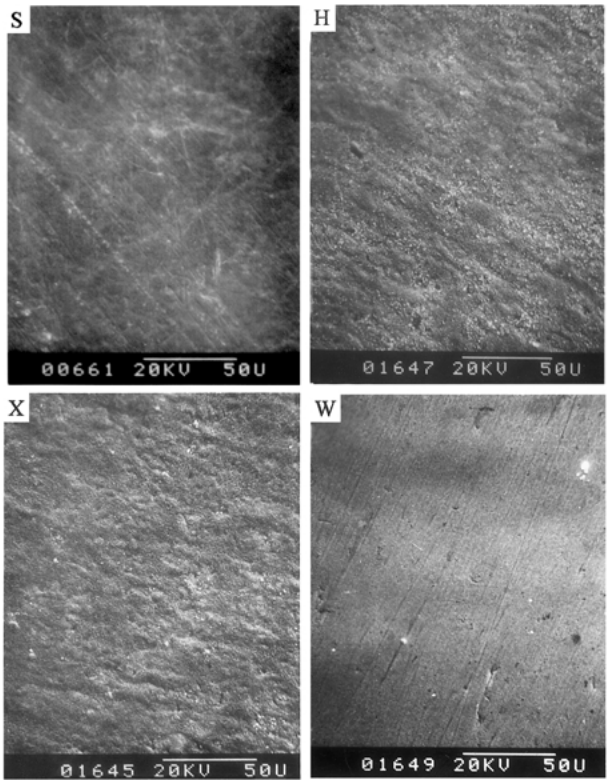

Figure 1 SEM micrographs of the titanium plates.

Binding energy peak area was derived using the Gauss curve-fitting routine to determine the percentage of the surface composition.

The crystal structure of the surface oxide films on titanium was identified using X-ray diffraction (XRD, improved D/max-RB, Japan) with CuKα radiation. Because the oxide films on titanium were so thin that X-ray could penetrate into the titanium substrate, sample tilting X-ray diffraction (ST-XRD) was also carried out for decreasing the diffraction intensity of titanium substrate and comparing with common Bragg X-ray diffraction (CB-XRD). The crystal structure of the coatings was investigated using X-ray diffraction (XRD, D/max-IIIA, Japan).

3. Results

3.1. Surface characterization of heat-treated samples

3.1.1. Morphology and surface roughness

Fig. 1 shows that the surfaces were uniformly roughened by heat-treatment, which was consistent with the measurement of surface roughness of the titanium plates (Fig. 2).

3.1.2. Surface energy

Fig. 3 shows that heat-treatment increased the surface energy of the samples. Heat-treatment in water vapor led to the highest surface energy. The change of the surface energy was attributed to the increase of the surface roughness which resulted in the increase of the specific surface area, and the variation of the surface compositions.

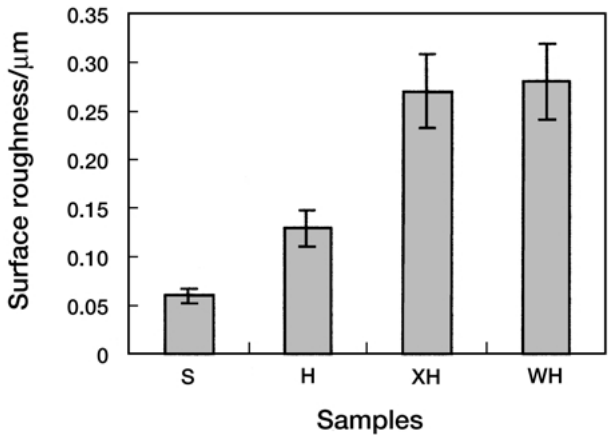

Figure 2 Surface roughness of the titanium plates.

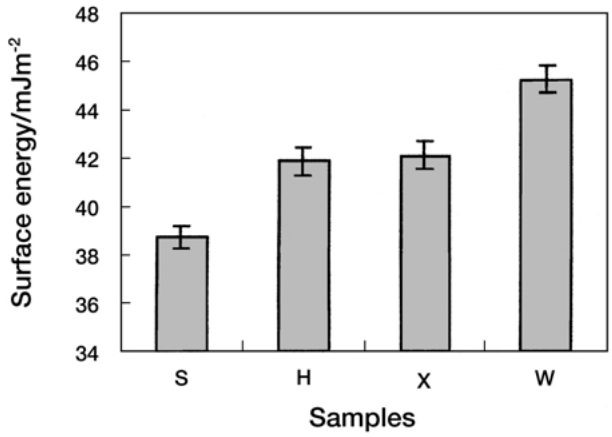

Figure 3 Surface energy of the titanium plates.

3.1.3. Surface crystal structure

Fig. 4 shows XRD patterns of samples. For S and W CB-XRD patterns were almost the same and there were only the peaks of titanium. For H and X, there were new peaks belonging to rutile TiO_2. This indicated that titanium was further oxidized during heat-treatment in both air and oxygen, and formed thick films of rutile instead of anatase. For S and W the oxide films were too thin to detect by XRD. But the oxide film of W could be assigned to rutile by XPS (see below).

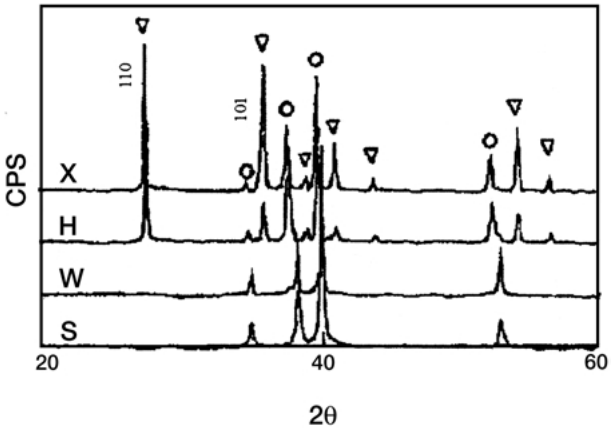

Figure 4 CB-XRD patterns of the titanium plates. ▽, rutile; ○, titanium.

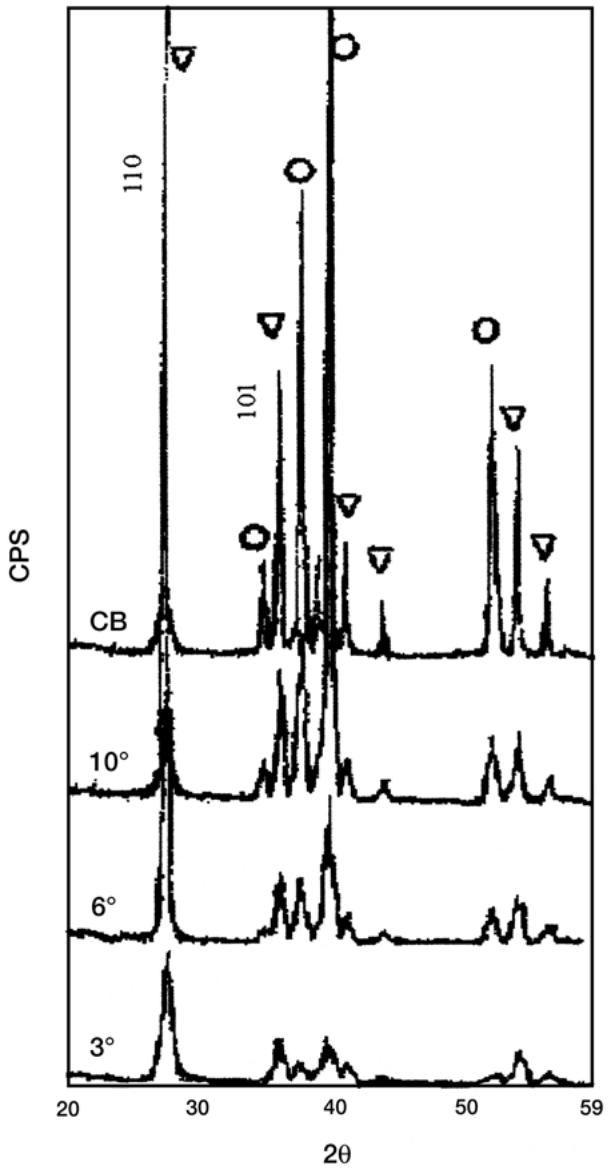

Figure 5 ST-XRD patterns of H. ▽, rutile; ○, titanium.

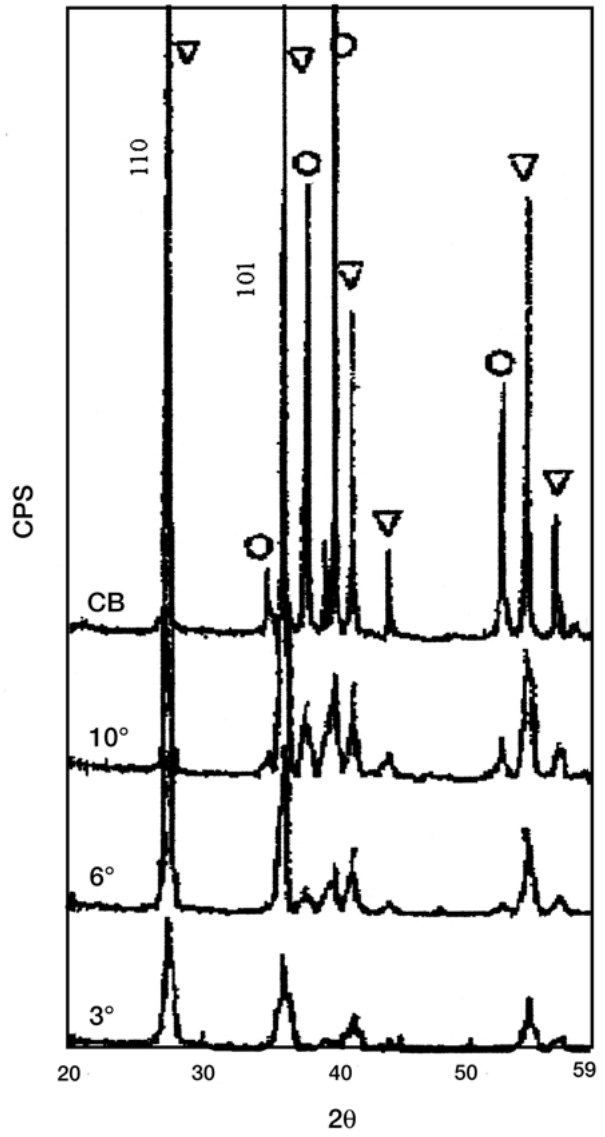

Figure 6 ST-XRD patterns of X. ▽, rutile; ○, titanium.

Figs. 5 and 6 show ST-XRD patterns of H and X in glancing angles of 3°, 6°, 10°, as the comparison, CB-XRD patterns are also given. In the oxide films there was only rutile. From the top surfaces to bulks (3°, 6°, 10° and CB-XRD), the intensity of titanium increased gradually, that is, the proportion of rutile decreased gradually. Comparing Fig. 5 with Fig. 6, the peak intensity of rutile of X was higher than that of H at all the angles. This indicated that thickness of rutile film of X was greater than that of H.

3.1.4. Surface compositions

Fig. 7 shows Ti2p and O1s spectra of titanium plates. For all the samples, the good symmetry of Ti2p spectra revealed that only, or at least predominantly, one kind of the oxidation state of titanium existed in the surface films. A difference between binding energies (ΔBE) of an O1s subpeak and $Ti2p_{3/2}$ peak for TiO_2 has been referenced to be 71.5 eV [13, 14]. The ΔBE of the four samples ranged from 72.0 to 72.3 eV. The small difference might be due to physisorbed water and chemisorbed water [15–17]. For H, X and W, the peak positions were very close to 458.1 eV binding energy of $Ti2p_{3/2}$ of rutile [3, 18]. That is, after different heat-treatments and then cooling to ambient temperature in air, the oxidation state of titanium in the surface films was almost the same, i.e. Ti^{4+} in rutile. This coincided well with the results of the XRD analyses.

The difference in O1s patterns among the four samples (Fig. 7) was mainly attributed to oxygen species on the surface films of titanium. According to Gauss curve-fitting routine, high-resolution spectral analysis was used for deconvoluting the O1s envelopes into three subpeaks: oxygen in TiO_2, in the physisorbed $(H_2O)_{ab}$ and acidic hydroxyl $(OH)_a$ groups, and in the basic hydroxyl $(OH)_b$ groups [16, 19, 20]. As an example, a curve fit for W is given in Fig. 8. The percentages of the three oxygen species obtained from the curve deconvolution are summarized in Fig. 9. Of the four samples, S surface had the highest percentage of TiO_2; W surface had the highest percentage of $(OH)_b$ groups; on H, X and W surfaces the percentages of $(H_2O)_{ab}$ and $(OH)_b$ groups were nearly equal and higher than that on S surface. In addition, Fig. 9 also indicated that heat-treatment increased the proportions of oxygen in the surface films.

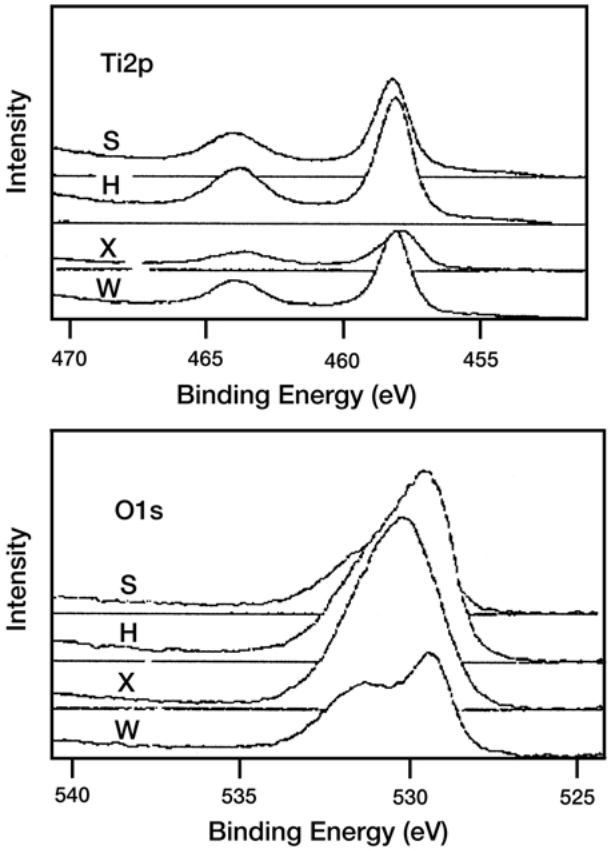

Figure 7 XPS spectra for Ti2p and O1s of titanium plates.

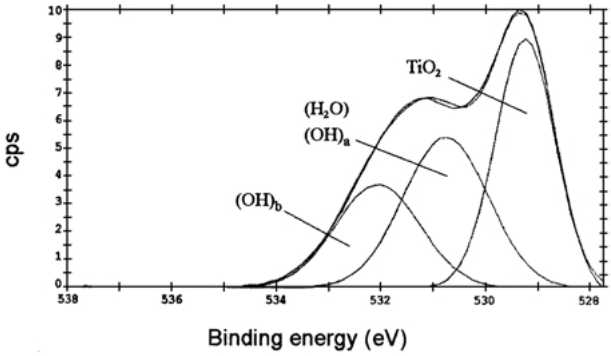

Figure 8 A representative XPS curve fit for O1s, taking W for example.

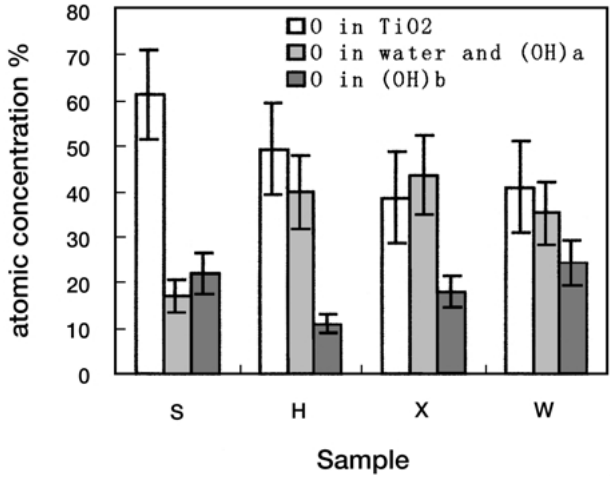

Figure 9 Percentages of three oxygen species on the surfaces of the titanium plates obtained by XPS.

3.1.5. ρ_{OH}

Fig. 10 shows the ρ_{OH} on the surfaces of the titanium powders. The ρ_{OH} on heat-treated powders (WP, HP and XP) were higher compared to non-heat-treated powder (SP). The analysis of BET method indicated that heat-treatments increased the specific surface areas of the powders, following the order of HP, XP and WP. Thus, the numbers on the total surface areas of the powders also increased, which was consistent with the XPS analysis for the percentages of $(OH)_s$ groups.

3.2. Formation of apatite coatings on the surfaces of heat-treated titanium

Fig. 11 is morphologies of the titanium plates heat-treated and then immersed in SCP for 10 days. On the surface of SS, scattered precipitants could be observed and no continuous film formed. On the surfaces of HS, XS and WS, crystal films could be observed. On WS a uniform and dense film covered the substrate. On HS the substrate was more clearly seen compared to XH. EDS analysis revealed an average Ca to P ratio of 1.57 in the precipitants.

Fig. 12 shows XPS spectra of immersed samples. Divalent calcium and phosphate ions were detected on all the samples, but the difference in peak intensities of calcium and phosphorous is significant. The intensities of Ca2p and P2p on WS surface are the highest, the ones on HS and XS surfaces are approximately equal, and SS had the lowest intensity. The Ca2p and P2p spectra for the four sample surfaces were a doublet with $Ca2p_{3/2}$ and $Ca2p_{1/2}$ at 346.90.2 eV and 350.30.2 eV, respectively. All the samples exhibited similar P2p spectra with a binding energy of 132.70 eV. This indicated that the precipitant on titanium was apatite [21, 22]. Fig. 13 is XRD patterns of immersed samples. Apatite was detected on WS. For XS, the peaks of apatite were very low. For HS, the peak was too low to differentiate from the background. For SS no apatite was detected by XRD. These were consistent with EDS results. In fact, the small amounts of calcium and phosphate on SS detected by XPS were not enough to detect by XRD and EDS. Although the uniformity of the coatings on XS was less than that on WS, the thickness of the apatite coating on XS was close to that on WS, about

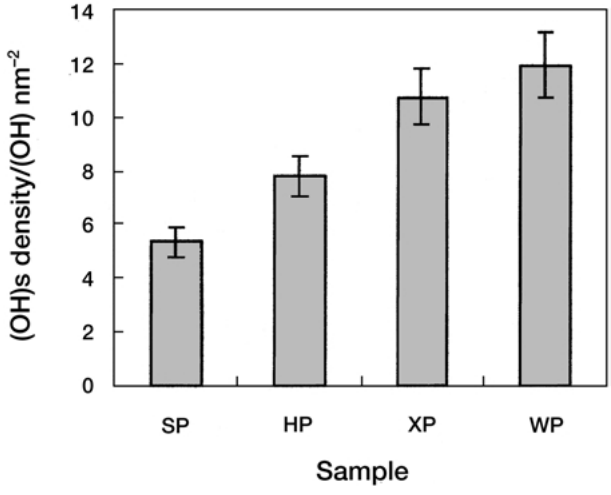

Figure 10 Densities of surface hydroxyl groups (OH/nm^2).

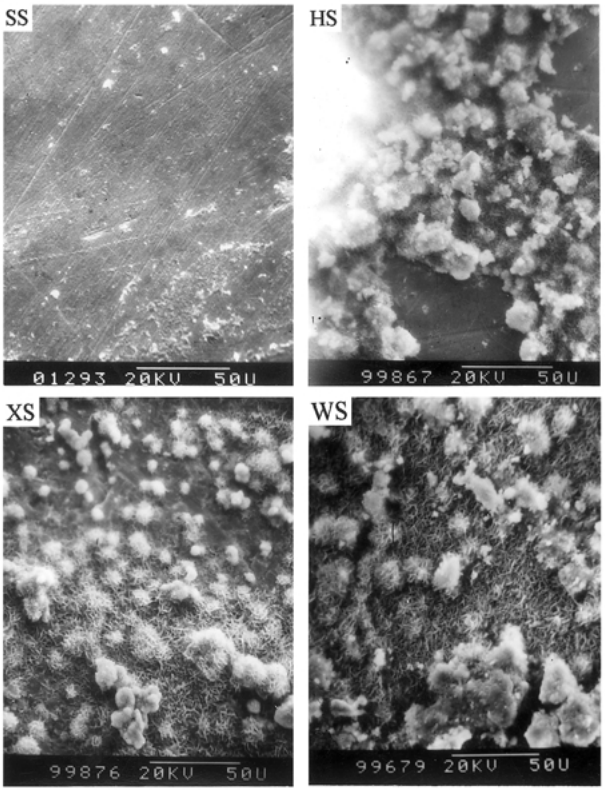

Figure 11 SEM micrographs of titanium plates heat-treated and then immersed in SCP for 10 days.

$1 \sim 3\,\mu m$. Fig. 14 shows the SEM micrograph of the cross-section of WS.

4. Discussion

Both XPS and XRD analyses showed that the surface oxide of heat-treated titanium was the rutile TiO_2. No suboxides of titanium were detected. From a chemical thermodynamic standpoint, the formation of rutile TiO_2 is a favorable process, since the Gibbs function of formation of rutile $(\Delta_f G^\circ_{m,298\,K} = -888.67\,kJ \cdot mol^{-1})$ is lower than that of anatase $(\Delta_f G^\circ_{m,298\,K} = -883.65\,kJ \cdot mol^{-1})$ [23]. In some cases, titanium suboxides, such as Ti_2O_3 and TiO could form [24–27]. However, in this study the sufficient oxygen at high temperature would convert titanium suboxides, even if they might instantaneously form, to TiO_2 with the highest oxidation state. This is because titanium has a strong affinity for oxygen, and TiO_2 is the most stable thermodynamically [2, 28].

It has been reported that hydrated surfaces of titanium contain more hydroxyl groups, thus improving the bioactivity of titanium [5, 8, 21, 29, 30]. Fig. 9 demonstrates that atomic ratios of O and Ti for the four samples were higher than 2. For S the ratio was slightly higher than 2. Heat oxidation enhanced the ratios. For X the ratio was the highest, up to 9.3. W and H had similar ratios, 3.2–3.5. The deviation from the stoichiometrical TiO_2 was attributed to $(H_2O)_{ab}$ and $(OH)_s$ groups. For non-heated sample (S), predominant TiO_2 with a little amount of $(H_2O)_{ab}$ and $(OH)_s$ groups existed on the surface, whereas for heated samples (H, W, X), mainly $(H_2O)_{ab}$ and $(OH)_s$ groups. During heat-treatment, oxygen and water reacted with the surfaces, resulting

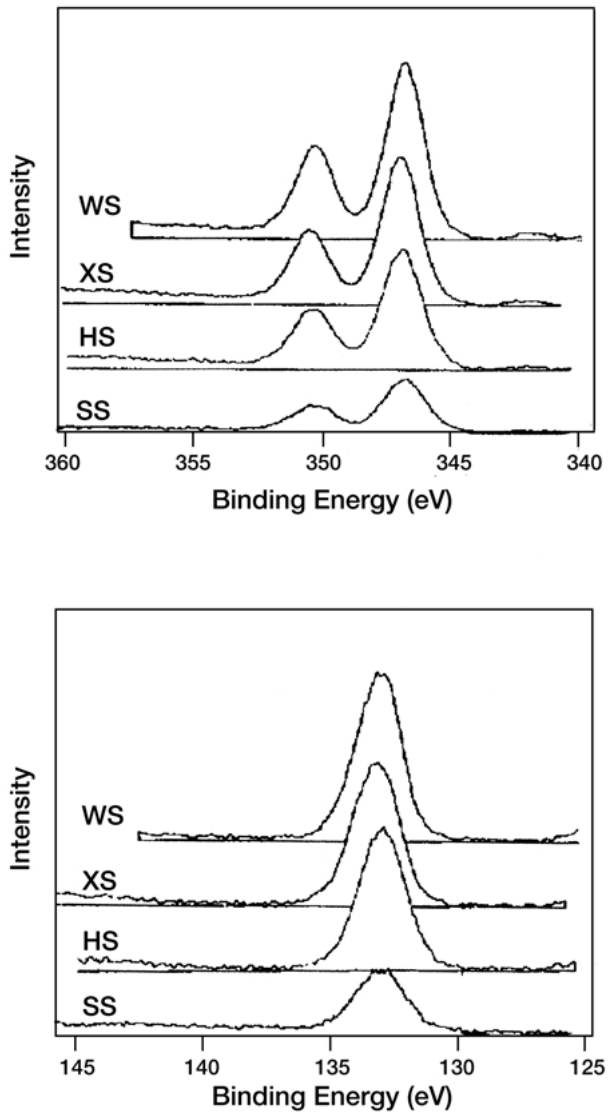

Figure 12 XPS Spectra for Ca2p and P2p of titanium plates heat-treated and then immersed in SCP for 10 days.

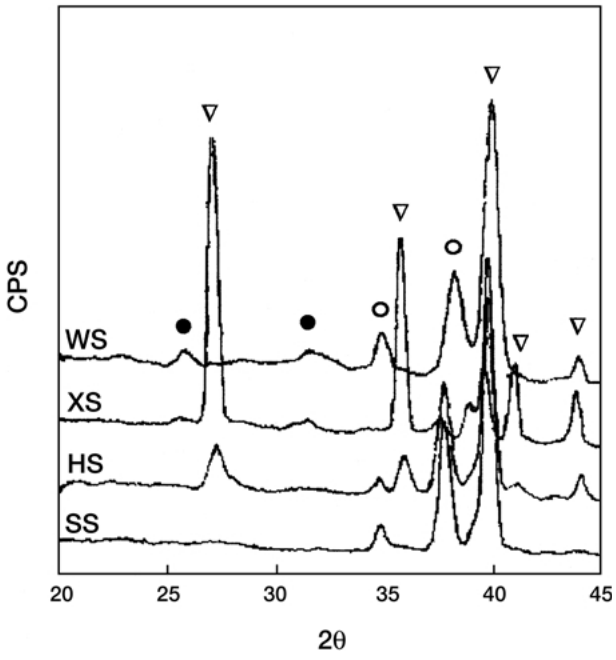

Figure 13 XRD patterns of titanium plates heat-treated and then immersed in SCP for 10 days. ●, apatite; ▽, rultile; ○, titanium.

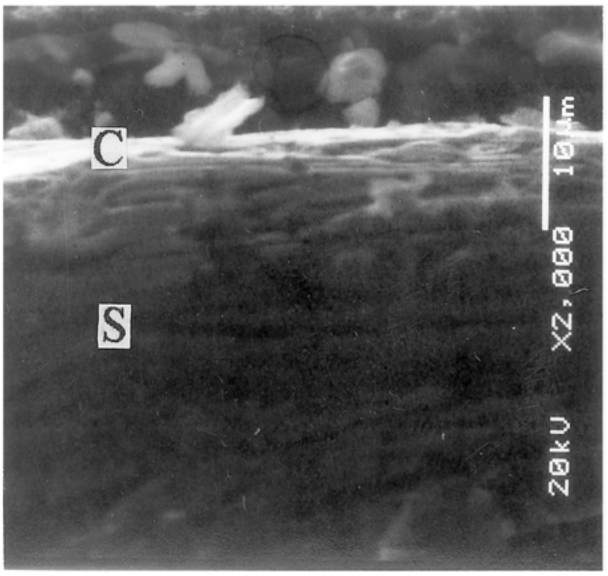

Figure 14 SEM micrograph of the cross section of WS. S, substrate; C, coating.

in the increase of the amount of $(OH)_s$ groups besides the thickening of the oxide films. The $(OH)_s$ groups, including the $(OH)_a$ and $(OH)_b$ groups originated from chemisorption. Since chemisorption belongs to monomolecular layer, when active sites on titanium surfaces which could induce chemisorption of water were saturated, the amount of hydroxyl groups would tend to be constant, thus the amounts of both $(OH)_a$ and $(OH)_b$ groups should be constant in given conditions. Besides monomolecular layer, generally, multimolecular layers could form by physisorption, which resulted in the increase of $(H_2O)_{ab}$ to a large extent. Probably, this process occurred mainly in the cooling, since physisorption is easier than chemisorption at low temperature. The variation of the percentages of $(OH)_s$ groups on the titanium plates was consistent with the analysis for the ρ_{OH} on the titanium powders (Fig. 10). The BET analysis indicated that heat-treatment increased the specific surface of the titanium powders and SEM analysis indicated that heat-treatment roughened the surfaces of the titanium plates. That is, heat-treated titanium plates had larger total surface areas compared to non-heat-treated titanium. Clearly, the larger surface areas would be beneficial to produce more active sites on the surfaces and active hydroxyl groups.

The patterns of CB-XRD and ST-XRD at 3°, 6°, 10° (Figs 4, 5 and 6) indicated that the crystal planes of rutile preferentially orientated in (1 1 0), next (1 0 1) at different depth in the films. The (1 1 0) plane of rutile has the highest atomic density ($10.2\,Ti/nm^2$), next, (1 0 1) plane ($7.9\,Ti/nm^2$) [31]. Higher density of titanium ions on the surfaces was responsible for more active sites. This orientation would favor the formation of more $(OH)_s$ groups.

The role of $(OH)_b$ groups in bioactivating titanium was often addressed by other researchers [5, 7, 8]. However, in the present study, the percentage of $(OH)_b$ groups on W was similar to that on S, whereas their bioactivity was obviously different. Compared to S, the percentages of $(OH)_b$ groups, $(OH)_a$ groups and $(H_2O)_{ad}$ on W surface were closer to those on H and X, which corresponded to the analysis for ρ_{OH} on the titanium powders, whereas the bioactivity of W was also more similar to H and X. This suggested that the bioactivity of the rutile films on titanium related to not only surface $(OH)_b$ groups but also $(OH)_a$ groups and the increasing of $(OH)_s$ groups on heat-treated titanium improved the reactivity of titanium. As a result, titanium was bioactivated and apatite spontaneously precipitated onto the surfaces in simulated biological environment. The amount of $(OH)_s$ groups on W were the highest, thus W showed the best bioactivity, as a result, the uniformity of apatite film on W surface was the best and the density the highest. That is, for bioactivating titanium, the heat-treatment in water vapor was superior to those in oxygen and air. This also suggested that the bioactivity of the rutile films was unrelated to their thickness.

Combining as mentioned above, it could be supposed that besides $(OH)_b$ groups, $(OH)_a$ groups and $(H_2O)_{ad}$ might also induce precipitation of apatite onto the rutile films. After heat-treatment, the bioactivated rutile surfaces might have three kinds of active sites. In biological environment, apatite might form on the titanium surfaces via the different active sites, as Fig. 15.

In another way, TiO_2 films on titanium formed naturally or obtained by sol–gel routine or anodic oxidation are all anatase. In this study, the rutile TiO_2 films were obtained by heat-treatment in different oxidation atmospheres and induced also the precipitation of apatite. So, both rutile and anatase could be bioactive in some conditions. The bioactivity of titanium would be unassociated with the crystal phase of surface TiO_2.

The effect of surface energy on biological properties has come into notice [32–34]. Fig. 3 indicated that heat-treatment increased the surface energy of titanium. This was possibly attributed to the change of the surface composition and the increase of the specific surface area. In the process of Ca-P precipitation, the variations of Gibbs function (ΔG) of the heat-treated samples (H, X and W) with higher surface energies should be greater, compared to that of non-heat-treated sample (S) with lower surface energy. The adsorption and reaction more easily occurred on their surfaces. Of all the samples, the titanium plates heat-treated in water vapor (W) had the highest surface energy and exhibited the best bioactivity. So, heat-treatment endowed titanium with the bioactivity to different extents by increasing the amount of surface hydroxyl groups and enhancing the surface energy of titanium.

5. Conclusions

In the surface oxide films of heat-treated titanium, rutile TiO_2 was predominant, and its crystal planes preferentially orientated in (1 1 0) plane with the highest density of titanium ions. This orientation would result in more surface active sites on titanium.

The rutile films on titanium could be bioactive in some conditions. The bioactivity of the rutile films was related to not only surface basic hydroxyl groups but also acidic hydroxyl groups and surface energy. Heat-treatment increased the percentages of surface hydroxyl groups on titanium and the values of surface energy, and thus endowed titanium with bioactivity. The treatment in

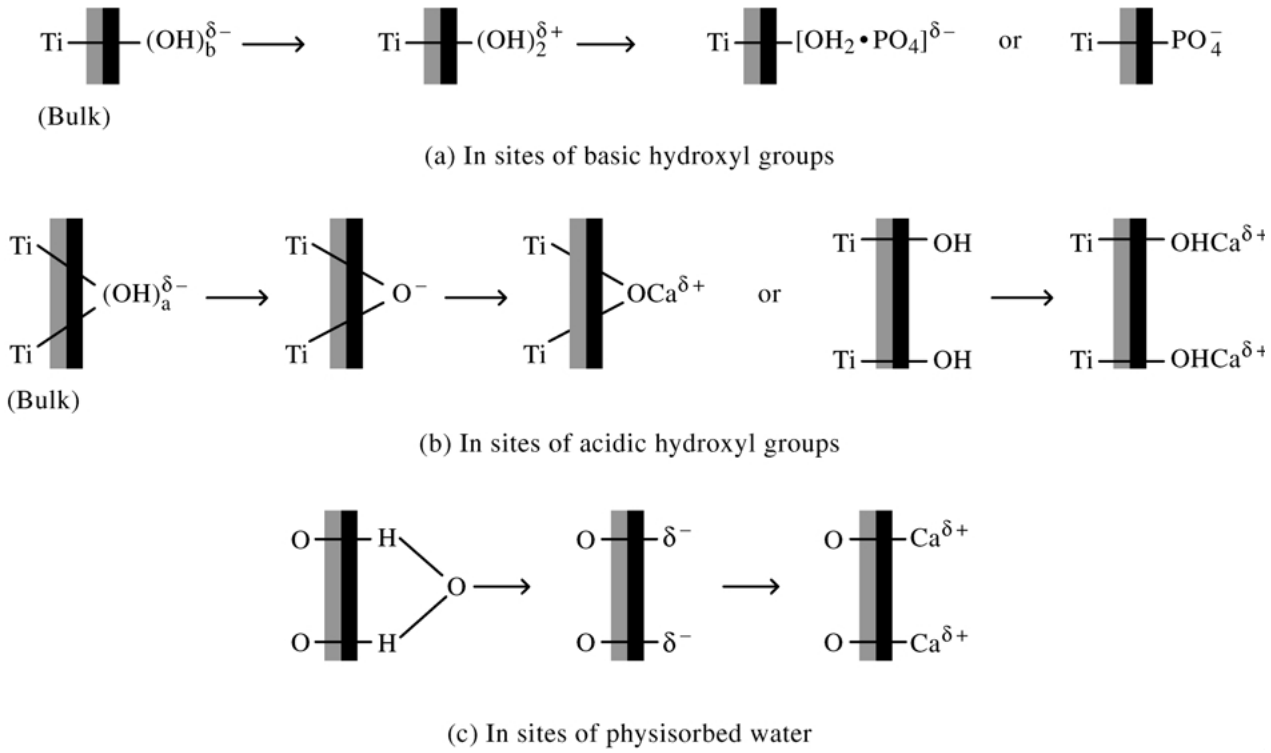

Figure 15 A supposed mechanism of approaching of calcium and phosphate ions to the surfaces of titanium via three active sites.

water vapor was better for bioactivating titanium compared to air and oxygen.

References

1. R. VAN NOORT, *J. Mater. Sci.* **22** (1987) 3801.
2. J. B. PARK and R. S. LAKES, in ''Biomaterials: An Indroduction'' (Plenum Press, New York, 1992) p. 89.
3. M. BROWNE and P. GREGSON, *J. Biomaterials* **15** (1994) 894.
4. M. SHIRKHANZADEH and S. SIMS, *J. Mater. Sci. Mater. Med.* **8** (1997) 595.
5. P. LI, K. DE GROOT and T. KOKUBO, *J. Am. Ceram. Soc.* **77** (1994) 530.
6. H. ISHIZAWA, M. FUJINO and M. OGINO, *J. Biomed. Mater. Res.* **29** (1995) 1459.
7. T. HANAWA and M. OTA, *Biomaterials* **12** (1991) 767.
8. C. OHITSUKI, H. IIDA, S. HAYAKAWA and A. OSAKA, *J. Biomed. Mater. Res.* **35** (1997) 39.
9. D. H. KAEBLE, *J. Adhesion* **2** (1970) 66.
10. D. K. OWENS and R. C. WENDT, *J. Appl. Polym. Sci.* **13** (1969) 1741.
11. A. KOZAWA, *J. Electreochem. Soc.* **106** (1959) 552.
12. T. HANAWA, M. KON, H. UKAI, K. MURAKAMI, H. HAMANAKA and K. ASAOKA, *J. Mater. Sci. Mater. Med.* **9** (1998) 89.
13. R. K. QUINN and N. R. AMOSTRING, *J. Electrochem. Soc. Electrochem. Sci. Technol.* **125** (1978) 1790.
14. J. L. ONG, L. C. LAUCAS, G. N. RAIKAR and J. C. GREGORY, *Appl. Surf. Sci.* **72** (1993) 7.
15. J. LAUSMAA, B. KASEMO and H. MATTSON, *ibid.* **44** (1990) 133.
16. K. E. HEALY and P. DUCHEYNE, *J. Biomed. Mater. Res.* **26** (1992) 319.
17. M. V. KUZNETSOV, F. J. ZHURAVLEV, V. A. ZHILYAEV and V. A. GUBANOV, *J. Electrn. Spectrosc. Relat. Phennom.* **58** (1992) 1.
18. M. BROWNE, P. J. GREGSON and R. H. WEST, *J. Mater. Sci. Mater. Med.* **7** (1996) 323.
19. T. K. SHAM and M. S. LAZARUS, *Chem. Phys. Lett.* **68** (1979) 426.
20. H. P. BOEHM, *Disc. Faraday Soc.* **52** (1971) 264.
21. S. A. REDEY, S. RAZZOUK, C. REY, D. BERNACHE-ASSOLLANT, G. LEROY, M. NARDIN and G. COURNOT, *J. Biomed. Mater. Res.* **45** (1999) 140.
22. L. J. ONG, V. A. HOPPE, H. L. CARDENAS, R. CAVIN, D. L. CARNES, A. SOGAL and G. N. RAIKAR, *ibid.* **39** (1998) 176.
23. R. C. WEAST (ed.) in ''CRC Handbook of Chemistry and Physics. 70th Edition, 1989–1990,'' (CRC Press Inc., Boca Raton, Florida, D-90).
24. B. F. LOWENBERG, S. LUGOWSKI, M. CHIPMAN and J. E. DAVIS, *J Mater. Sci. Mater. Med.* **5** (1994) 467.
25. B. W. CALLEN, B. F. LOWENBERG, S. LUGOWSKI, R. N. S. SODHI and J. E. DAVIS, *J. Biomed. Mater. Res.* **29** (1995) 279.
26. P. A. LEE, K. F. STORK, B. L. MASCHHOFF, K. W. NEBESNY and N. R. ARMSTRONG, *Surf. Interf. Analy.* **17** (1991) 48.
27. J. M. PAN, B. L. MASCHHOFF, U. DIEHOLD and T. E. MADEY, *J. Vac. Sci. Technol. A.* **10** (1992) 2470.
28. J. E. SUNDGREN, P. BODO and I. LUNDSTROM, *J. Collid. Interf. Sci.* **110** (1986) 9.
29. P. LI and K. DE GROOT, *J. Biomed. Mater. Res.* **27** (1993) 1495.
30. P. LI and P. DUCHEYNE, *ibid.* **41** (1998) 341.
31. P. JOENS and J. A. HOCKEY, *Trans. Faraday.* **67** (1971) 2679.
32. W. VAN DER VEGT, H. C. VAN DER MEI and H. J. BUSSCHER, *Langmuir* **10** (1994) 1314.
33. J. Y. MARTIN, Z. SCHWARTZ, T. W. HUMMERT, D. M. SCHRAUB, J. SIMPSON, J. LANKFORD JR, D. D. DEAN, D. L. COCHRAN and B. D. BOYAN, *J. Biomed. Mater. Res.* **29** (1995) 389.
34. M. LAMPIN, R. W-CLEROUT, C. LEGRIS and M. F. S-LUIZARD, *ibid.* **36** (1997) 99.

Received 2 June 2000
and accepted 19 August 2001